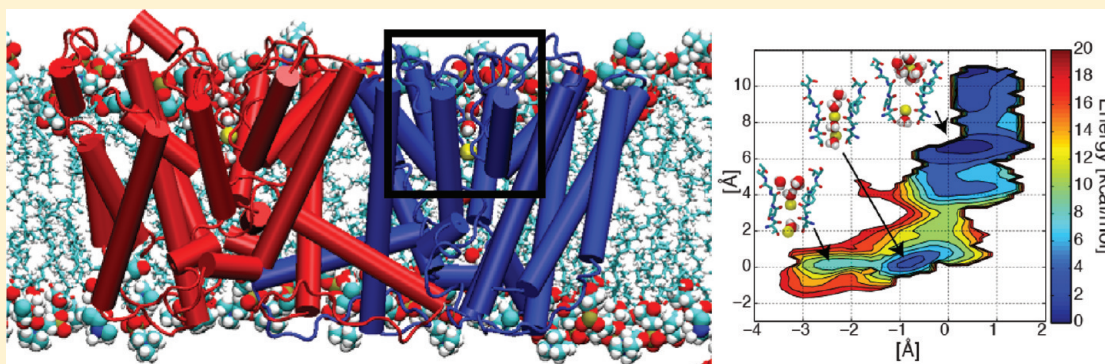


## Molecular Dynamics Simulations of the TrkH Membrane Protein

Carmen Domene<sup>\*,†</sup> and Simone Furini<sup>†,‡</sup><sup>†</sup>Physical and Theoretical Chemistry Laboratory, Department of Chemistry, University of Oxford, Oxford OX1 3QZ, U.K.<sup>‡</sup>Department of Medical Surgery and Bioengineering, University of Siena, viale Mario Bracci, 53100 Siena, Italy

## S Supporting Information



**ABSTRACT:** TrkH is a transmembrane protein that mediates uptake of  $K^+$  through the cell membrane. Despite the recent determination of its crystallographic structure, the nature of the permeation mechanism is still unknown, that is, whether  $K^+$  ions move across TrkH by active transport or passive diffusion. Here, molecular dynamics simulations and the umbrella sampling technique have been employed to shed light on this question. The existence of binding site S3 and two alternative binding sites have been characterized. Analysis of the coordination number renders values that are almost constant, with a full contribution from the carbonyls of the protein only at S3. This observation contrasts with observations of  $K^+$  channels, where the contribution of the protein to the coordination number is roughly constant in all four binding sites. An intramembrane loop is found immediately after the selectivity filter at the intracellular side of the protein, which obstructs the permeation pathway, and this is reflected in the magnitude of the energy barriers.

Potassium ions play pivotal roles in many physiological processes, as wide ranging as cell–cell communication, cell proliferation, and secretion. The intracellular concentration of  $K^+$  is generally much higher than that of the extracellular environment. Conversely, the extracellular fluid contains a concentration of  $Na^+$  ions as much as 10 times higher than that within the cell. Controlling these levels of ions is achieved through ion channels and transporters by means of passive and active transport, respectively. Transport proteins bind their substrates with high specificity but low energy barriers. In animal cells,  $K^+$  uptake is mainly achieved by the  $Na^+/K^+$ -ATPase.<sup>1</sup> In contrast, plants, bacteria, fungi, and archaea often have multiple  $K^+$  uptake systems, one of which is Trk. The Trk system is the major constitutive  $K^+$  uptake system of the bacterium *Escherichia coli*, with homologues found in many bacterial genomes. Four proteins are part of the Trk system: TrkH, TrkG, TrkA, and TrkE. TrkH and TrkG are transmembrane proteins, responsible for the transport of  $K^+$  across the cell membrane.<sup>2</sup> Both TrkH and TrkG coassemble with TrkA, which is a cytoplasmic protein with binding sites for NAD. In contrast, TrkE is an ATP-binding protein, necessary for the normal functioning of the TrkH–TrkA complex. The uptake of  $K^+$  through the TrkH–TrkA complex is sensible to intracellular NAD concentration, and it is thought to be linked

to  $H^+$  symport.<sup>3</sup> Despite the fact that the crystallographic structure of the TrkH protein was recently reported,<sup>4</sup> many questions about its permeation mechanism still remain open.

TrkH is a homodimer (see Figure 1). Each protomer is composed of five domains, named D0–D4. Domains D1–D4 have a  $K^+$  channel-like M1–P–M2 topology, and they arrange themselves around a pseudo-4-fold symmetry axis to form the ion conduction path. In contrast to  $K^+$  channels, domain D3 has also an intracellular loop that blocks the passage of ions.<sup>4</sup> The secondary structure of each P-loop resembles that of  $K^+$  channels, with a selectivity filter at the extracellular side of the pore (Figure 2). Each pore domain contributes to the selectivity filter with a different amino acid sequence; D1 contributes with TTTGAT, D2 with AIGGFS, D3 with TTAGFT, and D4 with>NNLGPG. The selectivity filter of TrkH may have evolved independently because of a requirement for  $K^+$  selectivity or may have a common ancestor with  $K^+$  channels in an archetypal  $K^+$  binding site.<sup>5</sup>

The extracellular region of TrkH is enriched by acidic residues, primarily aspartate amino acids (Figure 1B). Overall,

Received: October 15, 2011

Revised: February 7, 2012

Published: February 8, 2012

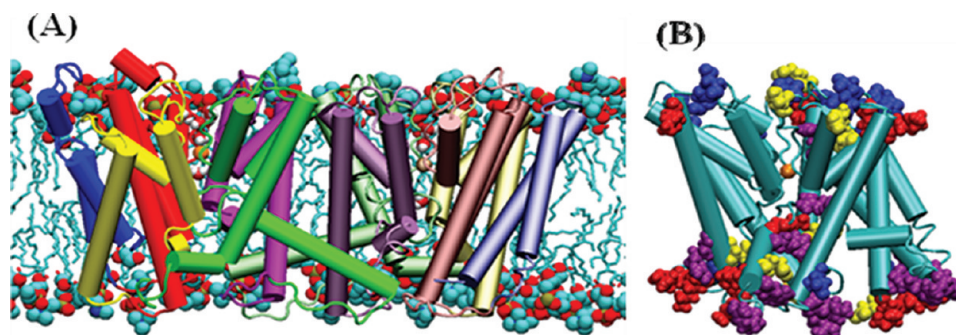


**Figure 1.** Structure of the TrkH protein. (A) Cartoon representation of the TrkH protein colored by domain and viewed from within the membrane. Protomer 1 is depicted in glossy colors and protomer 2 in metallic pastel colors using the same color scheme for the equivalent helices of each protomer. (B) Cartoon representation of protomer 1 of TrkH (cyan). Charged residues are shown in van der Waals representations: Glu (yellow), Asp (blue), Lys (red), and Arg (purple).

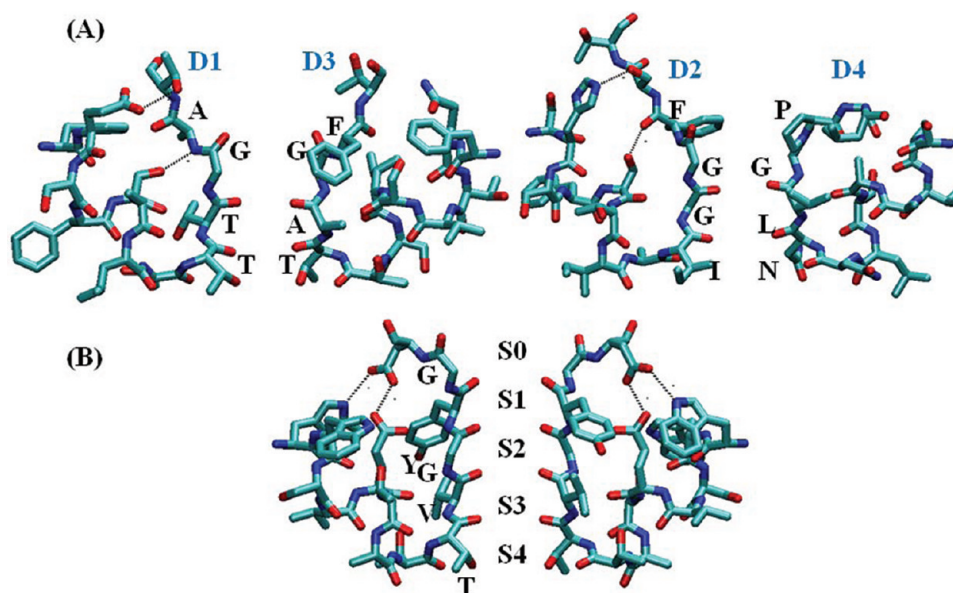


**Figure 2.** Selectivity filters of the TrkH transporter and the KcsA  $K^+$  channel and nature of the hydrogen bond network surrounding the selectivity filters. (A) Selectivity filter region and pore helix of two opposite subunits of TrkH. Some of the potential hydrogen bonds between the side chains or the pore helix residues and those of the selectivity filter are highlighted. (B) Selectivity filter region and pore helix of two opposite subunits of KcsA at high  $K^+$  concentrations. Residues 67–80 are shown as licorice. S0–S4 denote  $K^+$  binding sites. The hydrogen bonds between the side chain of Asp66 and Glu71 and between Asp66 and Trp67 are highlighted.

there are 16 aspartate residues; only three of them are on the intracellular side. There are nine glutamate residues equally arranged in the protein. One of them, Glu470, is strategically located at what seems to be the conduction pathway, and another, Glu104, is positioned behind what has been described as the selectivity filter. In total, these acidic residues account for 25 negative charges. In contrast, the intracellular region is enriched with basic residues. There are 16 arginine residues, one facing the extracellular solution (Arg32), another at the back of the selectivity filter (Arg131), and the rest on the intracellular side of the protein. One in particular, Arg468, is located in such a way that it will be in the proximity of the ions as they leave the selectivity filter. Twelve lysine residues are split evenly between the intracellular and extracellular regions of the protein, with the exception of one, Lys357, which is behind the intracellular circular loop.

The recent determination of the structure of TrkH from *Vibrio parahaemolyticus* at 3.51 Å resolution<sup>4</sup> provides an excellent opportunity for detailed computational and theoretical investigations of important aspects relating the structure and

function of TrkH such as permeation. Here, the permeation of  $K^+$  and  $Na^+$  ions through TrkH is analyzed by means of molecular dynamics (MD) simulations and free energy calculations. The adopted techniques have been widely used for the analysis of other membrane proteins. In the case of  $K^+$  channels, MD simulations revealed an atomistic description of ion permeation and selectivity.<sup>6</sup> Energy barriers for the permeation of  $K^+$  ions in  $K^+$  selective channels were found to be on the order of 2–3 kcal/mol.<sup>6e,7</sup> In contrast, a  $Na^+$  ion approaching a selectivity filter loaded with  $K^+$  ions experiences higher energy barriers, which prevents the passage of  $Na^+$  ions in  $K^+$  selective channels.<sup>6a,b</sup> More recently, atomistic simulations have been used to analyze ion conduction in the NaK nonselective channel, revealing energy barriers of 2–5 kcal/mol for the permeation of  $K^+$  and  $Na^+$  ions.<sup>6c</sup> The atomistic description of ion conduction in  $K^+$  and NaK channels provides an ideal starting reference for making a comparison with the permeation characteristics of TrkH. This could eventually provide new insights into the permeation mechanism of this membrane protein.

## MATERIALS AND METHODS

The atomic structure was defined according to Protein Data Bank entry 3PJZ.<sup>4</sup> All the residues of the two protomers determined in the X-ray structure were included in the atomic model. Channels were centered in the  $x$ - $y$  plane with the permeation pathway aligned with the  $z$ -axis and embedded in a pre-equilibrated bilayer of 632 1,2-dioleoyl-*sn*-glycero-3-phosphocholine molecules. The upper layer of the lipid membrane was aligned with the center of mass along  $z$  of the Tyr and Trp residues at the C-terminus of the outer helices. Lipid molecules closer than 1.2 Å to protein atoms were removed. The system was solvated with >20000 water molecules. Potassium and chloride ions were added to neutralize the system (to a final concentration of 150 mM). K<sup>+</sup> ions were placed at binding site S3 in both promoters, as in the X-ray structure. The total number of atoms in the system was ~125000. A second system in which the K<sup>+</sup> ions were replaced with Na<sup>+</sup> ions was defined. To equilibrate the atoms around the channels, 2000 steps of energy minimization and 500 ps of MD were performed, with restraints applied to the backbone atoms of the protein, and the ions in the filter. Restraints were initially set to 10 kcal mol<sup>-1</sup> Å<sup>-2</sup> and gradually reduced to zero. Two trajectories of 52 ns were generated with either K<sup>+</sup> or Na<sup>+</sup> ions occupying the selectivity filter of TrkH.

The potential of mean force (PMF) for K<sup>+</sup> and Na<sup>+</sup> ions inside the selectivity filter and their mixtures was calculated considering the motion of one or two ions, using the umbrella sampling technique.<sup>8</sup> These umbrella sampling simulations cover all the possible configurations of one ion, K<sup>+</sup> or Na<sup>+</sup>, or two ions, either two K<sup>+</sup> ions, two Na<sup>+</sup> ions, or one K<sup>+</sup> ion and one Na<sup>+</sup> ion, in the filter of TrkH. The collective variable for the one-dimensional (1D) umbrella sampling simulations was the distance along the  $z$ -axis between the center of the carbonyl oxygen atoms defining the binding site S3 and the ion traversing the selectivity filter. In the case of the two-dimensional (2D) umbrella sampling simulations, the collective variables were (1) the distance along the  $z$ -axis between the center of the carbonyl oxygen atoms defining the lower boundary of S3 and the bottom ion and (2) the distance along the  $z$ -axis between the center of the carbonyl oxygen atoms defining the upper boundary of S3 and the top ion. Collective variables were restrained by harmonic potentials with force constants of 10 kcal mol<sup>-1</sup> Å<sup>-2</sup>. The initial sets of umbrella sampling simulations were defined moving the center of the harmonic restraints with a step of 1 Å. Further umbrellas were added in infrequently sampled regions, using a higher force constant of 40 kcal mol<sup>-1</sup> Å<sup>-2</sup>, until a satisfactory overlapping among adjacent windows was reached. The starting structures were generated by systematically translating the ions to the center of the harmonic restraints and moving the surrounding water molecules accordingly. Approximately 30 and 100 windows per system were computed in the 1D and 2D sets, respectively. Each umbrella sampling simulation consisted of 2000 steps of energy minimization with restraints applied to the backbone atoms of the filter, followed by 1 and 0.5 ns of MD trajectory with harmonic restraints only on the ions, respectively, for the 1D and 2D sets. The first 20 ps was discarded as the equilibration period, and the remaining parts of the trajectories were used to calculate PMF with the weighted histogram analysis method.<sup>9</sup> Ions in both promoters were tracked in the umbrella sampling simulations, which provided two independent ion trajectories for each simulation. To

estimate the errors on the computed energies, the trajectories were divided into four separate data sets, i.e., first half and second half of the trajectories in promoters 1 and 2. The energy for each data set was calculated with the WHAM algorithm, and errors were estimated as the standard deviations between these values.

MD trajectories were simulated with NAMD version 2.7,<sup>10</sup> using the CHARMM27 force field with CMAP corrections,<sup>11</sup> and the TIP3 model for water molecules.<sup>12</sup> Parameters for K<sup>+</sup> and Na<sup>+</sup> ions inside the channel were defined according to ref 13. All the simulations were performed in the NpT ensemble. The pressure was maintained at 1 atm using a Nose-Hoover Langevin piston control,<sup>14</sup> with a period of 100 fs and a damping time constant of 50 fs. The temperature was maintained at 300 K by coupling to a Langevin thermostat, with a damping coefficient of 5 ps<sup>-1</sup>. Electrostatic interactions were treated with the particle mesh Ewald algorithm,<sup>15</sup> with a grid spacing of <1 Å. A smoothed cutoff (10–12 Å) was used for the van der Waals interactions. Equations of motion were integrated with a time step of 2 fs. The SETTLE algorithm was used to restrain hydrogen atoms.<sup>16</sup> In total, ~500 ns of MD trajectories was generated.

## RESULTS AND DISCUSSION

**Overall Stability of the Structure.** A simple measure of the drift in structure of the protein from its initial crystallographic conformation is provided by the root-mean-square deviation (rmsd) between the channel structure at a given time and the initial structure. Analysis of the  $\alpha$ -carbon rmsd for a dimer of protomers versus time revealed a similar pattern for each of the two simulations (with K<sup>+</sup> or Na<sup>+</sup> ions) over the 52 ns (see Figure S1 of the Supporting Information). There is a jump of ~1 Å at the start of each simulation followed by a small drift to a plateau value of ~2.5 Å, which is maintained for the remainder of the simulation. This initial structural drift is thought to reflect the fact that the restraints imposed during the equilibration period have been switched off and that the protein is free to relax within the lipid bilayer and the solvent. Analysis of the rmsd of individual helices and the helical component of the five different domains, D0–D4, shows that the rmsd values usually lie below 1 Å, with the exception of domains D0 and D2 of protomer 2 (Figure S2 of the Supporting Information). The movement of residues 117–123 of the second domain of protomer 2 is responsible for the jump observed in the rmsd. These residues are part of the loops of the protein on the extracellular side. The nature of the ions or their configuration in the selectivity filter does not influence the overall conformational stability of the protein on this time scale, as expected. In both protomers, the same pattern in the variation of the rmsd with respect to time can be observed. The rmsd values of the amino acids of the filter during the unrestrained trajectory oscillate between  $0.40 \pm 0.07$  and  $0.35 \pm 0.09$  Å for D1 and D3 and between  $0.73 \pm 0.11$  and  $0.76 \pm 0.26$  Å for D2 and D4.

Compared to the selectivity filter of K<sup>+</sup> channels,<sup>4</sup> the selectivity filter of TrkH has a wider opening on the extracellular side and a much shorter constricted region where ions are coordinated (Figure 2). The strength of the H-bond interaction between residues Glu71 and Asp80 behind the selectivity filter of KcsA is one of the key determinants of C-type inactivation.<sup>17</sup> It has also been shown that the H-bond pairing between residues Trp67 and Asp80, conserved in most K<sup>+</sup> channels, constitutes another critical interaction that



determines the rate and extent of KcsA C-type inactivation.<sup>18</sup> To test the role of the interactions between the pore helix and the outer vestibule of the TrkH transporter, we tracked several H-bonds during the S2 ns simulations (see Figure S3 of the Supporting Information). In domain D1, there is a H-bond between Glu104 on the pore helix and Val116 of the selectivity filter. In domain D2, there is a H-bond between Ser216 in the pore helix and Phe223. Additionally, a hydrogen bond interaction between His213 on the pore helix and Ser224 of the signature sequence is established in domain D2. Finally, in domain D3, a H-bond between Ser316 of the pore helix and Phe323 is present. Domain D4 lacks hydrogen bonds. This varied network is likely to stabilize the structure of the selectivity filter by contributing to a putative rigidity necessary to sustain precise carbonyl-ion coordination in the filter. Another interaction found in both protomers corresponds to that between Glu104 and Arg131 located at the back of the selectivity filter. During the simulations, these interactions always exist, which suggests that the hydrogen bond network behind the selectivity filter may also serve as a critical modulator of activation or gating besides its involvement in transport. However, in contrast to  $K^+$  channels where the critical binding site implicated in the mechanism of gating at the selectivity filter is site S2,<sup>6e,18,19</sup> in TrkH S2 is rather different from a structural point of view, and gating of the type described in  $K^+$  channels would not be feasible.

**Energy Profiles of  $K^+$  and  $Na^+$  Ions.** No ion transition was observed during the S2 ns of trajectory in either simulation or promoter.  $K^+$  or  $Na^+$  ions initially occupying binding site S3 remain at this site for the entire simulation. The only appreciable difference is that the  $K^+$  ion is coordinated by eight carbonyl oxygen atoms of the protein while the  $Na^+$  ion sits closer to the lower ring of carbonyls in S3 and is coordinated by five or six backbone carbonyl atoms of the protein. On the basis of the two simulations reported here, one is tempted to say that site S3 is particularly favorable for both  $K^+$  and  $Na^+$  ions in the filter of TrkH. However, more extensive simulations and detailed energetic analysis are required before any conclusions can be reached.

Figure 3 shows the free energy profile for the permeation of a single  $K^+$  or  $Na^+$  ion through the selectivity filter of the TrkH protein. The energy of permeation is shown as a function of the distance of the ion from the center of binding site S3. The lowest minimum for  $K^+$  permeation corresponds to a configuration in which the  $K^+$  ion occupies site S3. In site S3, the ion is coordinated by eight carbonyl oxygen atoms. The energy increases steeply for the inward movement of the  $K^+$  ion from S3 until it reaches the center of the ring defined by the carbonyl oxygen atoms delimiting sites S3 and S4. At this position, the  $K^+$  ion is coordinated by two water molecules in addition to the protein carbonyl oxygen atoms, and the energy is  $\sim 3$  kcal/mol higher than that at the global minimum. A configuration in which  $K^+$  occupies site S4 and the rest of the sites are occupied by water molecules is  $\sim 20$  kcal/mol less stable than the global minimum. The PMF of  $Na^+$  shows a minimum at which the ion occupies the ring defined by the carbonyl oxygen atoms delimiting the lower boundary of site S3, and a second local minimum ( $\sim 10$  kcal/mol higher in energy) with the ion at the ring defined by the carbonyl oxygen atoms delimiting the upper boundary of site S3. Energy barriers of  $>20$  kcal/mol block the exit of a  $Na^+$  ion from its minimal-energy configuration inside the selectivity filter. The movement of  $K^+$  and  $Na^+$  ions toward the intracellular side of the protein is

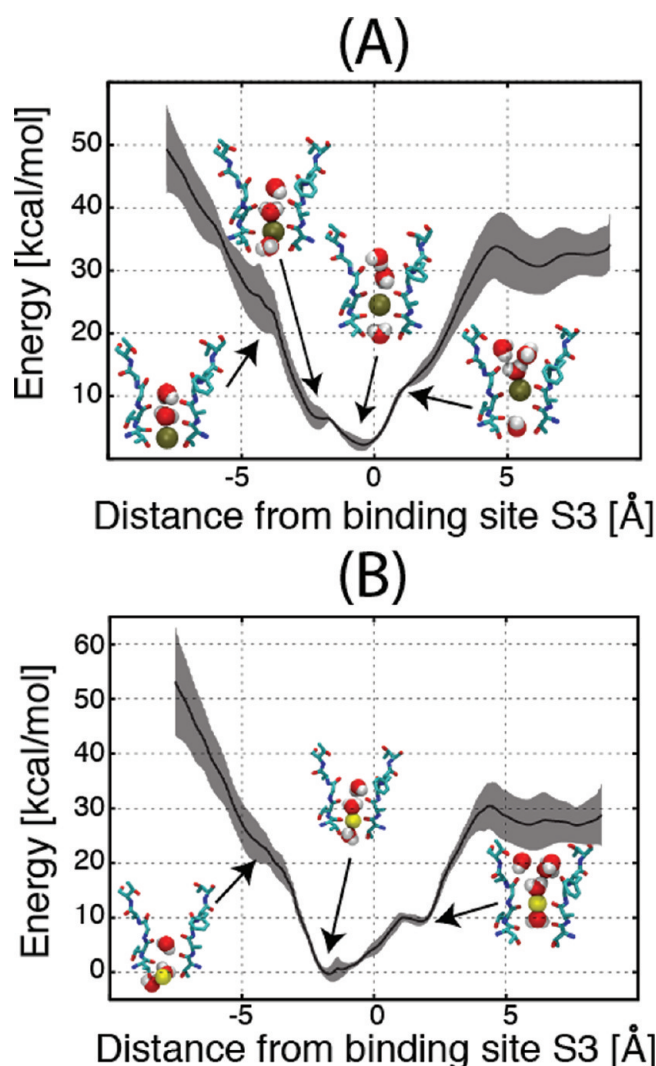


**Figure 3.** One-dimensional energy maps for conduction of  $K^+$  (A) and  $Na^+$  (B) ions in TrkH. Snapshots of the selectivity filter with the ion and nearby water molecules for the minima and other interesting situations are shown. The free energy profiles were computed as a function of the distance of the ion from binding site S3. Gray shading along the computed energy profiles is used to show the standard deviation.

blocked by the presence of a protein loop in the central cavity. At this point, an ion interacts with residue Thr352 of the protein loop of domain D3, which prevents further inward access (see Figure S4 of the Supporting Information). In the classical MD simulations, if all the frames are superimposed using the backbone atoms of the two promoters, the rmsd of the backbone atoms of the intracellular loop (residues 344–357) is  $1.1 \pm 0.2$  Å. This proves that the intracellular loop hardly moves inside the intracellular cavity, which is probably due to the limited space available.

Figure 4A shows the free energy profile for the permeation of two  $K^+$  ions through the selectivity filter of TrkH as a function of the displacement of the ions from the lower ( $x$ -axis) and upper ( $y$ -axis) boundary of site S3. Three minima can be characterized during the permeation events, the lowest of which corresponds to a situation in which  $K^+$  ions are at site S3 and on the extracellular side of the selectivity filter at different positions from the ion at site S3. This results in a rather broad minimum. Separated by a barrier of  $11 \pm 2$  kcal/mol, there is a

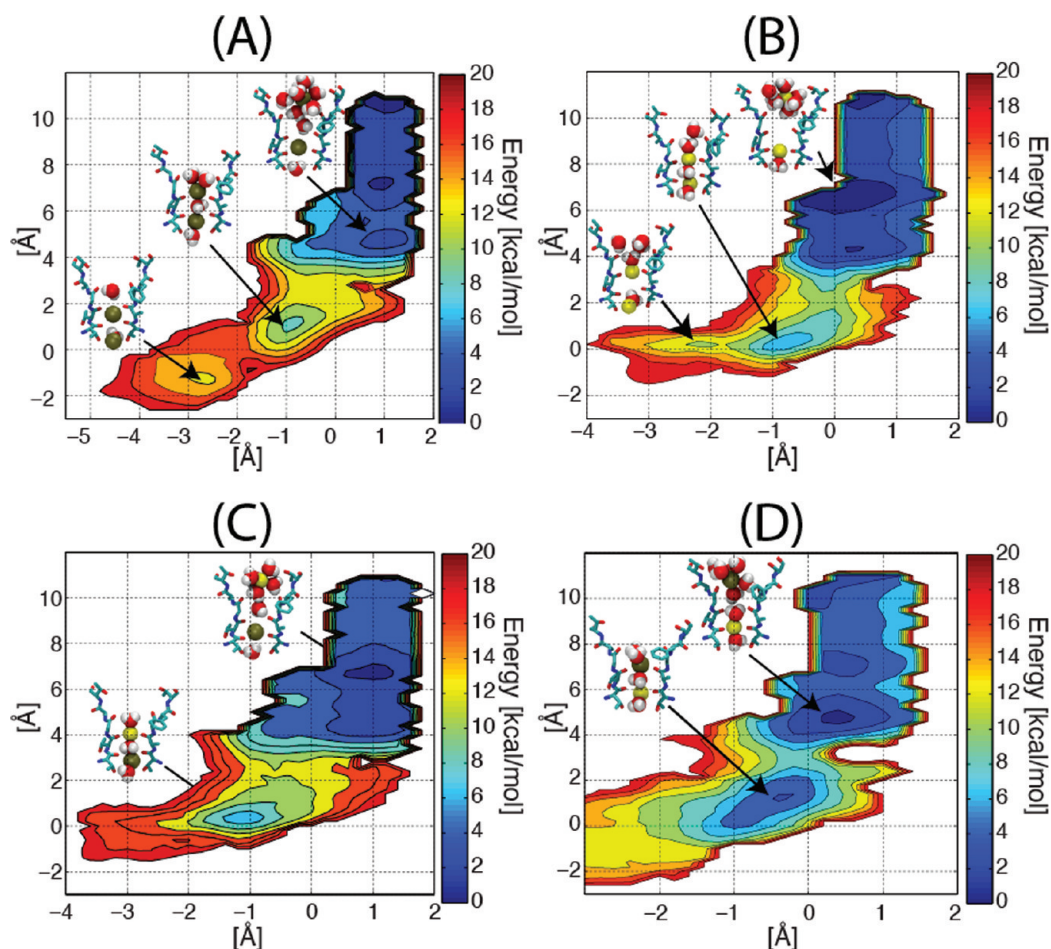


**Figure 4.** PMF for ion conduction in the TrkH protein. The free energy profile was computed as a 2D function of the displacement of one ion from the lower boundary of binding site S3 ( $x$ -axis) and the displacement of the second ion from the upper boundary of the same binding site. Contour lines are drawn every 2 kcal/mol. Snapshots of the selectivity filter corresponding to the local minima are shown for simulations with  $K^+$  ions (A),  $Na^+$  ions (B), and a mixture of ions (C and D). In panel C, the upper ion in the selectivity filter is  $Na^+$  and the lower ion is  $K^+$ . The order of the ions is reversed in the simulation shown in panel D.

second minimum that corresponds to a selectivity filter loaded with two ions, in sites S2 and S4, and a water molecule in site S3. The energy of this local minimum is  $8 \pm 2$  kcal/mol higher than the energy of the global minimum. A third minimum with an energy  $10 \pm 2$  kcal/mol higher than the global minimum corresponds to  $K^+$  ions at sites S3 and S4. Site S4 is rather broad, and a water molecule co-occupies this site with a  $K^+$  ion. A similar landscape and similar configurations can be detected during permeation of two  $Na^+$  ions through TrkH (Figure 4B). The global minimum corresponds to the selectivity filter with a  $Na^+$  ion at the center of the lower ring delimiting S3, and a second  $Na^+$  ion solvated in the extracellular solution. Like in the case of  $K^+$ , this minimum is rather broad and the width is correlated to the movement along the pore axis in the extracellular solution of the upper ion. Separated by a barrier of  $10 \pm 2$  kcal/mol, another minimum that characterizes a selectivity filter loaded with two  $Na^+$  ions, at site S4 and the upper ring of carbonyls of site S3, and a water molecule at S3, is found. A third local minimum,  $10 \pm 2$  kcal/mol higher than the global one, has an ion at the center of the upper ring defined by the carbonyl atoms of site S3 and a water molecule and an ion at site S4. The barriers for translocation of  $K^+$  and  $Na^+$  ions are similar,  $\sim 10$  kcal/mol. In the case of  $Na^+$  permeation, empty sites spontaneously appeared during the transport process.

These events were already described in the translocation of ions in  $K^+$  channels.<sup>6b,7b</sup>

Energy profiles of permeation of mixtures of  $K^+$  and  $Na^+$  ions were also considered with a  $K^+$  ion in an upper position in relation to the  $Na^+$  ion, and an alternative case with ions in reverse locations. The free energy surfaces describing the permeation of  $K^+/Na^+$  mixtures are characterized by two global minima (Figure 4C,D). One minimum corresponds to a configuration with a  $K^+$  ion at site S3 and a  $Na^+$  ion in the extracellular solution. In Figure 4C, a second minimum is observed separated by a barrier of  $12 \pm 3$  kcal/mol from the one previously described. It corresponds to a selectivity filter with a  $K^+$  ion at site S4 and a  $Na^+$  ion lying in the upper ring of carbonyls of site S3, with a water molecule at site S3. The lowest minimum in the translocation process with ions in reverse positions corresponds to a  $Na^+$  ion sitting in the lower ring of carbonyls of site S3 and the  $K^+$  ion in the extracellular solution. Water molecules occupy sites S2 and S4. The translocation toward a configuration with  $K^+$  and  $Na^+$  ions occupying the upper and lower rings, respectively, of carbonyl atoms of site S3 is hampered by an energy barrier of  $8 \pm 1$  kcal/mol (Figure 4D).

Like in the selectivity filter of  $K^+$  channels, main chain carbonyl oxygen atoms line the conduction pathway of the

TrkH protein, and by inspection, three ion binding sites equivalent to sites S2–S4 in K<sup>+</sup> channels can be defined and, potentially, host ions. The site equivalent to site S1 is lost because of the widening of the selectivity filter of TrkH. Experimentally, it was not possible to determine the contribution to the densities of K<sup>+</sup>, water, or other ions at these binding sites, because of the modest resolution of the crystallographic structure.<sup>4</sup> Only one site was confirmed by heavy atoms, equivalent to site S3 in K<sup>+</sup> channels. The energy analyses shown in Figures 3 and 4 support the hypothesis of three binding sites for K<sup>+</sup> ions in TrkH. Analysis of the coordination number in the trajectories generated in this study renders values of coordination numbers for K<sup>+</sup> ions of  $5.7 \pm 0.5$  and  $5.5 \pm 1.4$  in the simulations where two K<sup>+</sup> ions and one K<sup>+</sup> ion, respectively, are considered. Similarly, values of  $5.1 \pm 0.4$  and  $4.8 \pm 1.2$  are obtained in the simulations with two Na<sup>+</sup> ions and one Na<sup>+</sup> ion, respectively. In the simulations where both species are involved, the coordination numbers are  $5.8 \pm 0.6$  for K<sup>+</sup> and  $5.0 \pm 0.4$  for Na<sup>+</sup>. In all cases, the maximum of the number of protein atoms coordinating the ions or the minimum number of water molecules coordinating the ions, either K<sup>+</sup> or Na<sup>+</sup>, is at site S3 (see Figure S5 of the Supporting Information). At site S4, these values are reduced  $\sim 1.25$  units, and at site S2, the contribution coming from the protein is the same as that from water molecules. This differs from the situation observed in K<sup>+</sup> channels.<sup>6b</sup> The coordination number of the ions that travel across the TrkH selectivity filter is almost constant, and a full contribution of the carbonyl oxygen atoms of the protein is observed at only site S3. In contrast, in K<sup>+</sup> channels, the contribution of the protein to the coordination number is roughly constant in all four binding sites, with changes only at their boundaries.<sup>6b</sup> In general, the absolute values for the coordination numbers of both ions are larger in K<sup>+</sup> channels than in TrkH.

## CONCLUSIONS

Despite the fact that the crystallographic structure of the TrkH protein represents a landmark for the understanding of uptake of K<sup>+</sup> through the Trk complex, whether this protein operates as a transporter or as a channel remains an open question. In this study, classical MD has confirmed that a K<sup>+</sup> ion is stable at crystallographic binding site S3. From the analysis of the energies obtained with the umbrella sampling technique, two other binding sites for K<sup>+</sup> have been identified. Binding site S4 was already suggested by the crystallographic data, even if it was not possible to confirm its existence because of the modest resolution of the crystals. A comparison with the selectivity filter of K<sup>+</sup> channels also suggested the presence of a third binding site above site S3, and its presence was indeed confirmed by the free energy maps. From the local minima characterized in the energy map describing the conduction events for K<sup>+</sup> ions, a fourth site was observed  $\sim 5$  Å above the upper boundary of site S3. This binding site resembles the S<sub>ext</sub> binding site of K<sup>+</sup> channels, where the ion is coordinated essentially by water molecules.

In a filter occupied by a single K<sup>+</sup> ion, the ion in site S3 corresponds to the lowest-energy configuration, in agreement with the crystallographic data. By some means expected, removing the ion from site S3 is hampered by high energy barriers ( $\sim 20$  kcal/mol), excluding the possibility of a K<sup>+</sup> ion diffusing alone through the selectivity filter. These energy barriers for K<sup>+</sup> permeation could decrease as the result of two alternative mechanisms: (1) a structural change in the

selectivity filter that exposes binding site S3 alternatively to the extracellular or intracellular side or (2) the effect of an incoming ion that assists the movement of the ion already inside the filter, as described for K<sup>+</sup> channels. Here, we have tested the second hypothesis by calculating the energy maps of two ions moving through the selectivity filter. We found that the energy required to move a K<sup>+</sup> ion from site S3 to site S4 decreases by  $\sim 10$  kcal/mol. Progress toward the intracellular side is not possible because the central cavity is blocked by the presence of a loop from the protein, and this prevented us from simulating a complete conduction event. An energy barrier of  $\sim 10$  kcal/mol translates as follows: if two K<sup>+</sup> ions move through the selectivity filter of TrkH by passive diffusion, the conductance of this protein would be lower than that of K<sup>+</sup> channels, where lower energy barriers between 2 and 3 kcal/mol have been described.<sup>6b,c,20</sup> However, the single-channel conductance of TrkH is unknown, and the involvement of a third K<sup>+</sup> ion could further decrease the energy barriers of the permeation process presented here. Transport could proceed through various steps with ions in the following positions: S3/S<sub>ext</sub>/extracellular, S4/S2/S<sub>ext</sub> and intracellular/S3/S<sub>ext</sub>. The obstruction of the permeation pathway below the selectivity filter by the protein loop prevented us from testing this hypothesis. In a manner independent of the permeation mechanism, active transport or passive diffusion, the protein loop occupying the central cavity needs to be displaced to allow the passage of ions through TrkH. This structural change could be mediated by TrkA or triggered by protons moving across the protein.

Polarization effects have often been suggested as being important in the transport of ions in ion channels.<sup>13,21</sup> A shortcoming of this study is the fact that the force field parameters used for protein–water, water–ion, and protein–ion interactions, do not allow for a consideration of polarization effects, a limitation shared with a number of other studies. In the absence of a fully developed polarizable force field for water, ions, protein, and lipids, this study represents an attempt to delineate some of the main features of ion permeability in the TrkH membrane protein.

## ASSOCIATED CONTENT

### Supporting Information

C<sub>α</sub> atom root-mean-square deviations (Figure S1), contributions of the structural elements to the C<sub>α</sub> atom root-mean-square deviation (Figure S2), snapshots illustrating some of the hydrogen bond interactions observed during the molecular dynamics simulations (Figure S3), blockage of ion conduction by a protein loop in the intracellular cavity (Figure S4), and coordination numbers of Na<sup>+</sup> or K<sup>+</sup> ions in various simulations (Figure S5). This material is available free of charge via the Internet at <http://pubs.acs.org>.

## AUTHOR INFORMATION

### Corresponding Author

\*Physical and Theoretical Chemistry Laboratory, Department of Chemistry, University of Oxford, South Parks Road, Oxford OX1 3QZ, U.K. Telephone: +44-1865285401. Fax: +44 1865 275410. E-mail: [carmen.domene@chem.ox.ac.uk](mailto:carmen.domene@chem.ox.ac.uk)

### Funding

The EPSRC UK National Service for Computational Chemistry Software is acknowledged for providing computational resources. Part of the work has been performed as part of



Project HPC-EUROPA2 (Project 228398), with the support of the European Community, under the FP7 'Research Infrastructures' Programme. C.D. thanks The Royal Society for a University Research Fellowship.

# Notes

The authors declare no competing financial interest.

# REFERENCES

- (1) Skou, J. C. (1998) The influence of some cations on an adenosine triphosphatase from peripheral nerves (Reprinted from *Biochim. Biophys. Acta*, vol 23, pg 394–401, 1957). *J. Am. Soc. Nephrol.* 9 (11), 2170–2177.
- (2) Bakker, E. P. (1993) *Low-affinity K<sup>+</sup> uptake systems*; CRC Press, Boca Raton, FL.
- (3) Rhoads, D. B., and Epstein, W. (1977) Energy coupling to net K<sup>+</sup> transport in *Escherichia coli* K-12. *J. Biol. Chem.* 252 (4), 1394–1401.
- (4) Cao, Y., Jin, X. S., Huang, H., Derebe, M. G., Levin, E. J., Kabaleswaran, V., Pan, Y. P., Punta, M., Love, J., Weng, J., Quick, M., Ye, S., Kloss, B., Bruni, R., Martinez-Hackert, E., Hendrickson, W. A., Rost, B., Javitch, J. A., Rajashankar, K. R., Jiang, Y. X., and Zhou, M. (2011) Crystal structure of a potassium ion transporter, TrkH. *Nature* 471 (7338), 336–340.
- (5) Maser, P., Hosoo, Y., Goshima, S., Horie, T., Eckelman, B., Yamada, K., Yoshida, K., Bakker, E. P., Shinmyo, A., Oiki, S., Schroeder, J. L., and Uozumi, N. (2002) Glycine residues in potassium channel-like selectivity filters determine potassium selectivity in four-loop-per-subunit HKT transporters from plants. *Proc. Natl. Acad. Sci. U.S.A.* 99 (9), 6428–6433.
- (6) (a) Nimigeon, C. M., and Allen, T. W. (2011) Origins of ion selectivity in potassium channels from the perspective of channel block. *J. Gen. Physiol.* 137 (5), 405–413. (b) Furini, S., and Domene, C. (2011) Selectivity and Permeation of Alkali Metal Ions in K<sup>+</sup>-channels. *J. Mol. Biol.* 409 (5), 867–878. (c) Furini, S., and Domene, C. (2011) Gating at the selectivity filter of ion channels that conduct Na<sup>+</sup> and K<sup>+</sup> ions. *Biophys. J.* 101 (7), 1623–1631. (d) Furini, S., Beckstein, O., and Domene, C. (2009) Permeation of water through the KcsA K<sup>+</sup> channel. *Proteins* 74 (2), 437–448. (e) Berneche, S., and Roux, B. (2001) Energetics of ion conduction through the K<sup>+</sup> channel. *Nature* 414 (6859), 73–77. (f) Khalili-Araghi, F., Tajkhorshid, E., and Schulten, K. (2006) Dynamics of K<sup>+</sup> ion conduction through Kvl1.2. *Biophys. J.* 91 (6), L2–L4.
- (7) (a) Aqvist, J., and Luzhkov, V. (2000) Ion permeation mechanism of the potassium channel. *Nature* 404 (6780), 881–884. (b) Furini, S., and Domene, C. (2009) Atypical mechanism of conduction in potassium channels. *Proc. Natl. Acad. Sci. U.S.A.* 106 (38), 16074–16077. (c) Domene, C., and Furini, S. (2009) Dynamics, energetics, and selectivity of the low-K<sup>+</sup> KcsA channel structure. *J. Mol. Biol.* 389 (3), 637–645.
- (8) (a) Torrie, G. M., and Valleau, J. P. (1974) Monte-Carlo free-energy estimates using non-Booltzman sampling: Application to subcritical Lennard-Jones fluid. *Chem. Phys. Lett.* 28 (4), 578–581. (b) Domene, C., and Furini, S. (2009) Examining ion channel properties using free-energy methods. *Methods Enzymol.* 466, 155–177.
- (9) Kumar, S., Bouzida, D., Swendsen, R. H., Kollman, P. A., and Rosenberg, J. M. (1992) The weighted histogram analysis method for free-energy calculations on biomolecules. 1. The method. *J. Comput. Chem.* 13, 1011–1021.
- (10) Phillips, J. C., Braun, R., Wang, W., Gumbart, J., Tajkhorshid, E., Villa, E., Chipot, C., Skeel, R. D., Kale, L., and Schulten, K. (2005) Scalable molecular dynamics with NAMD. *J. Comput. Chem.* 26 (16), 1781–1802.
- (11) MacKerell, A. D., Bashford, D., Bellott, Dunbrack, R. L., Evanseck, J. D., Field, M. J., Fischer, S., Gao, J., Guo, H., Ha, S., Joseph-McCarthy, D., Kuchnir, L., Kuczera, K., Lau, F. T. K., Mattos, C., Michnick, S., Ngo, T., Nguyen, D. T., Prodhom, B., Reiher, W. E., Roux, B., Schlenkrich, M., Smith, J. C., Stote, R., Straub, J., Watanabe, M., Wirkiewicz-Kuczera, J., Yin, D., and Karplus, M. (1998) All-atom

empirical potential for molecular modeling and dynamics studies of proteins. *J. Phys. Chem. B* 102 (18), 3586–3616.

(12) Jorgensen, W. L., Blake, J. F., and Buckner, J. K. (1989) Free energy of TIP4P water and the free-energies of hydration of CH<sub>4</sub> and Cl<sup>−</sup> from statistical perturbation theory. *Chem. Phys.* 129 (2), 193–200.

(13) Roux, B., and Berneche, S. (2002) On the potential functions used in molecular dynamics simulations of ion channels. *Biophys. J.* 82 (3), 1681–1684.

(14) Feller, S. E., Zhang, Y. H., Pastor, R. W., and Brooks, B. R. (1995) Constant-pressure molecular dynamics simulation: The Langevin piston method. *J. Chem. Phys.* 103 (11), 4613–4621.

(15) Essmann, U., Perera, L., Berkowitz, M. L., Darden, T., Lee, H., and Pedersen, L. G. (1995) A smooth particle mesh Ewald method. *J. Chem. Phys.* 103 (19), 8577–8593.

(16) Miyamoto, S., and Kollman, P. A. (1992) Settle: An analytical version of the Shake and Rattle algorithm for rigid water molecules. *J. Comput. Chem.* 13 (8), 952–962.

(17) Cordero-Morales, J. F., Cuello, L. G., Zhao, Y., Jogini, V., Cortes, D. M., Roux, B., and Perozo, E. (2006) Molecular determinants of gating at the potassium-channel selectivity filter. *Nat. Struct. Mol. Biol.* 13 (4), 311–318.

(18) Cordero-Morales, J. F., Jogini, V., Chakrapani, S., and Perozo, E. (2011) A multipoint hydrogen-bond network underlying KcsA C-type inactivation. *Biophys. J.* 100 (10), 2387–2393.

(19) (a) Morais-Cabral, J. H., Zhou, Y. F., and MacKinnon, R. (2001) Energetic optimization of ion conduction rate by the K<sup>+</sup> selectivity filter. *Nature* 414 (6859), 37–42. (b) Domene, C., Klein, M. L., Branduardi, D., Gervasio, F. L., and Parrinello, M. (2008) Conformational changes and gating at the selectivity filter of potassium channels. *J. Am. Chem. Soc.* 130 (29), 9474–9480.

(20) Furini, S., and Domene, C. (2009) Atypical mechanism of conduction in potassium channels. *Proc. Natl. Acad. Sci. U.S.A.* 106 (38), 16074–16077.

(21) (a) Allen, T. W., Kuyucak, S., and Chung, S. H. (1999) Molecular dynamics study of the KcsA potassium channel. *Biophys. J.* 77 (5), 2502–2516. (b) Kuyucak, S., Andersen, O. S., and Chung, S. H. (2001) Models of permeation in ion channels. *Rep. Prog. Phys.* 64 (11), 1427–1472. (c) Illingworth, C. J., and Domene, C. (2009) Many-body effects and simulations of potassium channels. *Proc. R. Soc. London, Ser. A* 465 (2106), 1701–1716. (d) Illingworth, C. J. R., Furini, S., and Domene, C. (2010) Computational studies on polarization effects and selectivity in K<sup>+</sup> channels. *J. Chem. Theory Comput.* 6 (12), 3780–3792.